01

Machine-learned interatomic potential of Li−C for nanomaterials

© S.A. Sozykin

South Ural State University
(National Research University),
454080 Chelyabinsk, Russia
e-mail: sozykinsa@susu.ru

Received October 2, 2024
Revised October 2, 2024
Accepted October 2, 2024

The paper reports on the development of two types of interatomic interaction potentials for the atomistic modelling of carbon nanomaterial complexes with lithium. The first potential is constructed using the Gaussian approximation method and the second using the deep learning approach. These potentials have been trained using the results of density functional modelling and provide an accuracy close to that of this method with significantly lower computational requirements. The datasets contained more than 8000 structures of about 100 atoms. A given structure was placed in the training set with 90 % probability, otherwise it was placed in the validation set. The resulting potentials allow accurate reproduction of the energies of the complexes and the forces acting on the atoms. The computation time increases linearly with the number of atoms in the model and can vary by several orders of magnitude depending on the type of potential and the hardware used. The potential obtained by the deep learning method seems promising for realistic and accurate modelling of lithium on the surface of carbon nanotubes and various graphene-like structures at temperatures up to 450 K.

Keywords: molecular dynamics, deep learning, regression, lithium, carbon nanomaterials.

DOI: 10.61011/TP.2025.03.60844.292-24

Introduction

Explosive growth of demand for portable sources of energy caused active research of carbon nanostructures as a material of lithium battery anode [1]. The experiment shows that using a multi-layer graphene in the battery anode [2] or carbon nanotubes (CNT) [3] instead of graphite makes it possible to increase its reversible lithium capacity. In case of vertically-aligned CNTs [4] the path of lithium diffusion inside the anode does not cause doubts contrary to the graphene, which may have a scaly structure that promotes lithium adsorption along the scale boundaries. Such uneven distribution of lithium on the surface may cause low sensitivity of the process of intercalation to the concentration of graphene defects [5].

To understand the processes happening in the anode of the lithium battery in discharging/charging processes, the realistic models are necessary — digital twins of such anodes. Such models may not be based only on quantum-mechanical methods due to the complexity of the anode structure, and, accordingly the large size of the estimated cell. For example, the promising material of the battery anode proposed in paper [6] is a graphene grown on the CNTs that are covalently connected to graphene. Paper [7] describes the promising outlook of using the CNTs grown on graphene as anodes of lithium-sulphur batteries. Paper [8] reports the achievement of the outstanding characteristics of the battery when using a composite material containing CNTs as an anode. These examples show that the structure of the promising materials is much more complicated as the arrays of nanotubes or stacks of graphene sheets. It is evident that such materials contain carbon with various hybridization and are built not only from carbon hexagons. Therefore, the relevant objective becomes to study the lithium behavior near the surface of the carbon nanomaterials joined in a complicated manner and to develop the corresponding modeling methods.

The common theoretical approach to study of the lithium adsorption on the carbon surfaces is the electronic density functional theory. It has an undeniable advantage: there is practically no need for a priori information on the studied system, and the validity of the obtained results is limited only by the available computing resources. The latter circumstance noticeably limits the size of the model available for the study. The alternative is classic molecular dynamics with interparticle potentials of interaction, which depend on several parameters. These parameters may be selected based on various assumptions, but the obtained potential turns out to be applicable only for a narrow class of objects (close to those systems, for which the parameters were adjusted).

The quantum jump in improvement of forecasts of the „classic“ modeling may be obtained using the methods of artificial intelligence, where the potential is built using the estimate data by the electronic density functional theory (DFT), but not as an explicit function, but as a neuron network. This is a very rapidly developing area of research opening the possibility to do modeling by method of classic molecular dynamics with the accuracy not inferior to the method of non-empirical molecular dynamics. Obviously, DFT is successfully used to adjust the potential parameters without use of the artificial neuron networks as

Table 1. Parameters c of graphite cell AB-and length of bonds C−C, L_{C-C}, obtained using various exchange-correlation functionals (EX)

EX	L_{C-C}, Å	c, Å	EX	L_{C-C}, Å	c, Å
LDA	1.412	6.588	vdW-DF-cx of Berland and Hyldgaard	1.426	6.833
PBE	1.424	7.852	SCAN+rVV10 of Peng	1.416	6.627
PBE-D3	1.423	6.905	rVV10 of Sabatini	1.424	6.348
optB88-vdW	1.424	6.638	r^2SCAN+rVV10 of Ning	1.418	6.620
optB86b-vdW	1.423	6.566	Original vdW-DF of Dion	1.430	7.076
rev-vdW-DF2	1.423	6.595	optPBE-vdW of Klimeš	1.427	6.792
vdW-DF2 of Lee	1.429	6.943	Experiment	1.418	6.708

well. The example may be the GAP potentials (Gaussian Approximation Potentials) [9].

Currently several implementations of the machine-trained potentials are known, the objective of which is to replace the DFT method for large-scale and long estimations. The most common of them are the following — MLIP (Machine Learning Interatomic Potentials) [10], DP (Deep Potentials) [11] and CHGNet (Crystal Hamiltonian Graph neural Network) [12]. All the listed models were developed in the last decade and are currently being actively developed. All of them may be used together with the LAMMPS software for modeling by the method of classic molecular dynamics.

The obvious success in the development of the machine training methods related to atomistic modeling would be even more evident for the scientific community, if more ready-to-use interparticle potentials were available. For example, there are universal potentials for carbon [13,14], for 2D carbon structures [15], for carbon structures with account of Van der Waals interaction [16,17], the development of DP-potential is reported [18] (the potential itself is unavailable). For the lithium and carbon systems there is only potential [19] (used together with [13]).

This study is aimed at building potential DP-to describe the interaction of lithium with the surface of CNT and graphene-like structures. Potentials and examples of input files for LAMMPS software with their use are given in additional materials to this paper.

1. Method

Most machine training models, including DP and GAP, suggest that the potential energy of the system may be presented by a sum of energy contributions of each atom describing multiple interactions between the atoms within a certain fixed distance. This approach is convenient from the computing point of view, since its complexity rises linearly with the system size. In many cases the neglection of the far-reaching Coulomb interaction causes no large errors. In part it is due to the fact that the models are trained on the DFT modeling results that take into account the electrostatic interaction. For those rare cases, when such indirect accounting is not sufficient, there are generalizations of the machine training method for the accurate accounting of the far-reaching electrostatic interactions [20].

The consequence of the specified feature in the machine-trained potentials is the presence of a certain cutoff radius, the impact of atoms beyond which is neglected. To exclude the non-physical interactions, the translation parameters must be twice higher than the doubled cutoff radius. When selecting the cutoff parameter, it is useful to take into account the specific scales of interactions in the system. Thus, the covalent interactions C−C are observed at distances of less than 0.16 nm. At distances of around 0.36 nm only low Van der Waals interactions are observed in the graphite. Lithium in the main state is located at the distances of around 0.25 nm from the carbon surface. In this paper the cutoff radius was selected as equal to 0.6 nm.

All results of quantum-chemical calculations given in this paper were generated in VASP software [21]. It is known that there are problems with description of the graphite layers interaction in DFT [22]. The parameter c of graphite cell AB-and length of bond C−C, L_{C-C} in it produced when using some exchange-correlation functionals are given in table 1. From the table you can see that most functionals overestimate the length of bond C−C compared to the experimental value. Nevertheless, the deviations do not exceed 0.012 Å. The situation is worse with parameter c of the lattice: the PBE functional most often mentioned in the scientific articles causes a substantial re-estimation of this value. Using the empirical correction PBE-D3 improves the situation, but its empirical nature prevents from being confident in the correctness of correction prediction to the energy of more complicated carbon nanomaterials with lithium compared to graphite. The situation is complicated by the fact that the structures, on which the potential is trained, must be far from the balance: the forces that the atoms are exposed to are practically zero for the equilibrium structures, which reduces the volume of useful data for potential training. From table 1 you can see that there is a whole range of functionals that describe well both interatomic and interplanar spacing in graphite. Unfortunately , using all of them, except for the excessively simplified functional of LDA is linked to colossal computing expenses compared to PBE, which prevented the review of the models discussed in this paper on the computing resources available to the author. In connection with the above, the calculations in this paper were carried

out using exchange-correlation functional of PBE. The calculations were carried out without accounting for spin using pseudopotential PAW. The cutoff energy was selected as equal to 600 eV. The break of the reciprocal space into k-points was done using the Monkhorst–Pack scheme with various parameters for unidimensional $(1 \times 1 \times 29)$ and two-dimensional $(6 \times 6 \times 1)$ models, which provide for convergence with respect to energy of not below 0.1 meV/atom.

The potentials were developed with two independent tools: DeePMD-kit (v2.2.6) [11] and GAP [23]. The first of them suggests deep training (artificial neuron networks with hidden layers), and the second one, to develop the potential, uses non-parametric regression, which does not suggest a closed functional shape and does not attempt to explain the process that the data are based on, using theoretical assumptions: the flexible function is adjusted using large data volumes [24]. Identical training and validation data sets were submitted to the input of both programs, which contain coordinates and type of atoms, the forces they are exposed to, energies of the systems and virials (the sum taken with a reverse sign for all atoms of the system of scalar products of the atom radius-vector and the force that the atom is exposed to).

It should be noted that the preparation of machine-trained potentials requires substantial computing resources. In case of a GAP potential, computing nodes are required with high volume of random access memory (hundreds of gigabytes / node). To train the quality DP-potentials, the powerful video cards of supercomputer level are required: Tesla P100, Tesla V100, Tesla A100 etc .

To train the potential using DeePMD software, for comparison the se_e2_a and se_e3 descriptors were used. Both these descriptors are related to „Smooth Edition“ version of descriptors. For descriptors of this type, two concentric spheres are identified, in the center of which a specific atom is located. The cutoff sphere with the large radius limits the area of the space, the interaction with atoms in which is taken into account when training the potential. Besides, interaction with the atoms inside the small sphere is taken into account in full, and with the atoms in the area between the spheres with the weight reducing to zero in the large radius sphere. Abbreviations e2 and e3 specify that the first of them takes into account the two-particle interactions, and the second one — interactions of atom triplets. However, it does not mean that the se_e2_a descriptor takes into account only the distances between the atoms. It takes into account their mutual location (radius-vector).

Most parameters of the se_e2_a and se_e3 descriptors match each other. In this paper the values for them were also selected the same. The cutoff radius was specified as equal to 0.6 nm, besides, the descriptor would gradually decrease, starting from the distance of 0.4 nm. The maximum quantity of the considered carbon and lithium atoms in the environment of this atom was set as equal to 160 and 80 accordingly. This parameter was selected based on the assumptions that the quantity of the carbon atoms limited by the sphere of radius 0.6 nm, in the tightest package is around 160. There are much less lithium atoms in the system. The hidden network contained three layers with size of 50, 100 and 200. The adjustable network contained three layers, each with size of 250. The final speed of training was 10^{-8}, the training was done for the duration of 10^6 epochs. The final weights of energies, forces and virial in the function of losses made 1.5, 1.0 and 0.2 accordingly. Besides, the variant of joint use of se_e2_a and se_e3 descriptors with the reduced cutoff radius for se_e3 was considered.

To develop the GAP-potential, the distance_Nb descriptors of the second and third orders, the SOAP descriptor were used. All parameters for these descriptors were taken from paper [19] with some exceptions for the SOAP descriptor: n_max and l_max parameters were specified as equal to 9, the cutoff parameter was equal to 4.0 nm (maximum value at which the calculation would start in four computing nodes with 250 GB random access memory on each one). Therefore, the characteristics of the structure within a certain sphere surrounding a specific atom were:

1) distances between atoms (two-particle descriptor);

2) angles formed by atom triplets (three-particle descriptor);

3) complex information on the mutual position of atoms (multi-particle SOAP descriptor).

SOAP descriptor for each atom is a vector of hundreds of components (thousands for the systems with several elements). Their quantity depends on several parameters, which, if selected properly, may achieve substantial reduction in data submitted to the input of the training procedure without damage to the quality of the trained potential. Use of the SOAP descriptor makes it possible to substantially improve the quality of the obtained potential and increases the computing resources required for its training by far.

2. Results and discussion

2.1. Training, validation and test sets

Creation of the structures database was done in several stages. At the first stage a small number (around 100) of steps *ab-initio* of the molecular dynamics of carbon nanostructure models was placed into the base (nanotube, graphene, biphenylene, irida-graphene, ψ-graphene, tetra-penta-deca-hexagonal graphene) with lithium, the examples of which are given in fig. 1. The models contained around 100 atoms of carbon and up to 10 atoms of lithium. Such concentrations correspond to „gas“ and „islands“ of lithium on the carbon surface [25]. New structures were added according to the algorithm DP-Gen [26] from the molecular-dynamic modeling at temperatures of up to 450 K. The elementary cell size was maintained as equal to 2.5 nm in the directions perpendicular to the axis of the nanotubes, and in the direction perpendicular to the plane of graphene-like structures. Other translation

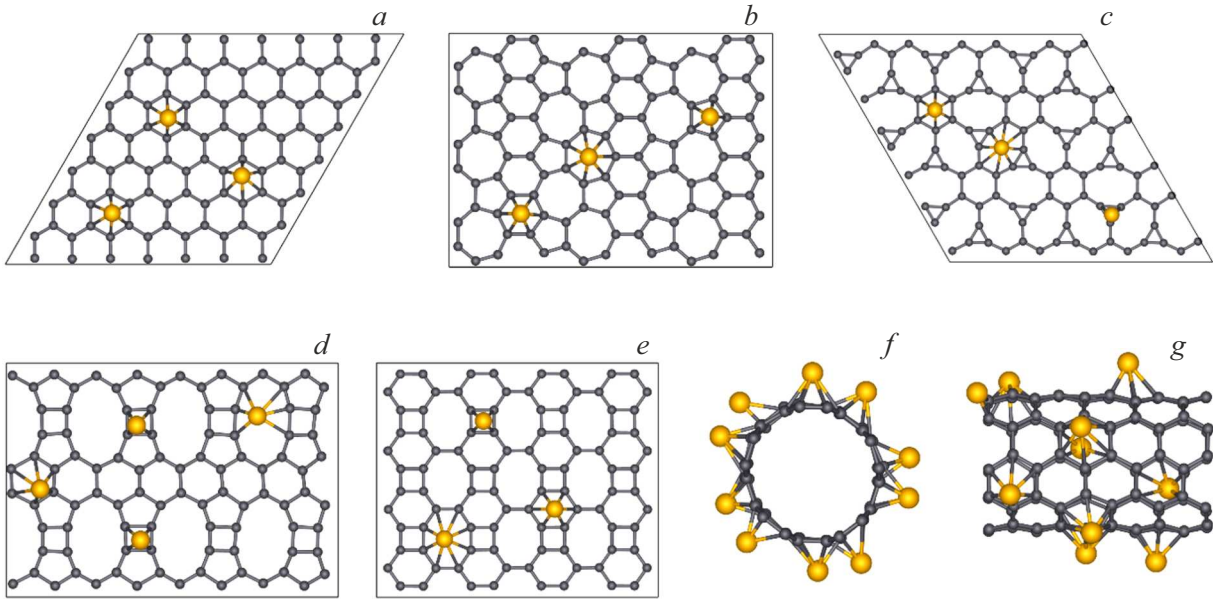

Figure 1. Representatives of model classes: *a* — graphene+3Li, *b* — PSI-graphene+3Li, *c* — irida-graphene+3Li, *d* — tetra-penta-deca-hexagonal graphene+4Li, *e* — biphenylene+3Li, *f*, *g* — CNT(5,5)+10Li.

parameters were taken from the corresponding step of the molecular dynamics. Therefore, the base of the structures describes the nanotubes and graphene-like objects that do not interact with their periodical images. After the base was increased several times, the initial structures obtained in the method of molecular dynamics were excluded from the base. Therefore, all structures in the base were selected by DP-Gen. The database contained 8723 structures, including 513 structures without a lithium atom (63 CNT(5,5), 50 of graphene, 100 of biphenylene, 100 of irida-graphene, 100 of ψ-graphene and 100 of tetra-penta-deca-hexagonal graphene), 778 CNT(5,5)+1Li, 328 CNT(5,5)+5Li, 1498 CNT(5,5)+10Li, 209 graphene+1Li, 230 graphene+3Li, 1262 biphenylene+3Li, 1342 irida-graphene + 3Li, 1211 ψ-graphene + 3Li, 1356 tetra-penta-deca-hexagonal graphene+4Li and one structure of the isolated lithium atom.

A specific model with probability of 90 % was placed into a training sample, otherwise it would get into a validation sample. The test sample was formed by two data sets:

1) 70 structures with a lithium atom on a straight line perpendicular to the hexagon of the nanotube wall and passing through its center (fig. 2, *a*);

2) 30 structures with a lithium atom on a straight line parallel to graphene with the shortest distances to the centers of hexagons corresponding to the equilibrium distance from lithium to graphene (fig. 2, *b*).

2.2. Potential quality assessment

The root mean squared error (RMSE) is often a quantitative measure of errors that the machine training model tries to minimize. To assess the accuracy of the potential vs the various types of the structures, RMSE were calculated on the validation base. The results for the four potentials are given in table 2 for each class of objects. DP-e2, DP-e3 and DP-hybrid mean the potentials produced for the cases of using the se_e2_a, se_e3 and hybrid descriptors, accordingly. You can see that the hybrid potential causes least errors. Maximum errors occur when the se_e3 descriptor is used. Both specified potentials turned out to be much more demanding to computing resources compared to the potential DP-e2. We will consider it further in this paper. In its case in seven out of ten cases the error turns out to be less than 1 meV/atom. For the three remaining ones — less than 2 meV/atom. For RMSE forces — it does not exceed 0.115 eV/Å. GAP potential provides for accuracy comparable to the DP potentials only for one system (CNT(5,5) with five lithium atoms). In other cases the errors turn out to be up to several times higher. This indicates the complexity of obtaining high quality GAP-potentials for the case of large variety of the models in the training and test samples. This fact will not reflect the principal limitation of the GAP approach, but only demonstrates the limited nature of the computing resources available to the author.

According to RMSE estimates (table 2), the produced PD potentials are not inferior to the ones given in literature. For quartz glass the least RMSE of energy and force made 4 meV/atom and 0.289 eV/Å accordingly [27]. The larger RMSE (4.1 meV/atom) was obtained for gold clusters of similar structure [28]. The attempt of training using the more diverse gold clusters, the error increased by far. DP-potential trained on a set from multiple carbon materials [18], generates RMSE 17 meV/atom for the validation sample from graphene structures. Error estimates are substantially smaller in case of model training in single-type structures [29]. Therefore, the DP potentials obtained in

Table 2. Estimation of accuracy of DP-potentials on validation and test sets of data

Class of systems		DP-e2		DP-hybrid		DP-e3		GAP	
Carbon surface	n_{Li}	RMSE of energy, meV/atom	RMSE of force, meV/Å	RMSE of energy, meV/atom	RMSE of force, meV/Å	RMSE of energy, meV/atom	RMSE of force, meV/Å	RMSE of energy, meV/atom	RMSE of force, meV/Å
CNT(5,5)	1 (inside tube)	0.32	49	0.28	50	0.32	83	1.07	55
CNT(5,5)	1 (out tube)	0.43	68	0.42	71	0.77	114	2.63	74
CNT(5,5)	5	1.69	101	1.63	99	2.23	137	2.10	109
CNT(5,5)	10	1.50	111	1.49	109	2.07	147	5.59	120
Graphene	1	2.37	65	2.08	59	2.96	82	12.50	49
Graphene	3	3.36	64	2.57	60	2.08	85	8.58	54
Biphenylene	3	0.86	93	0.77	84	0.80	133	6.75	91
Irida-graphene	3	1.05	97	0.64	76	1.11	117	9.08	82
ψ-graphene	3	1.04	79	0.86	72	1.29	122	5.72	75
Tetra-penta-deca-hexa-gonal graphene	4	0.89	87	0.73	74	1.58	140	2.44	87
Test set 1	1	4.75	95	3.14	89	5.38	156	3.12	60
Test set 2	1	3.35	20	3.31	18	3.63	21	12.67	14

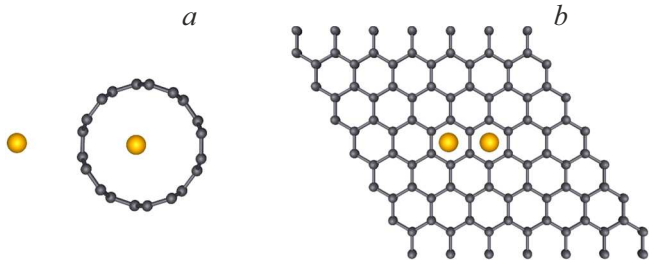

Figure 2. End positions of lithium atom in test sets: *a* — 1 and *b* — 2.

this paper may be recommended for use when studying the complexes of various carbon surfaces with lithium atoms. Despite the fact that the estimates of errors for various classes of models differ, all of them are small compared to typical errors reported in the literature for such potentials.

Note that for the DP potential case you can only decide on the quality of the potential based on the RMSE dependence on the epoch, which DeePMD software generates in process of training, in the case when the structures used for training are described well enough by the potential in every case. The thing is that the specified data are calculated not for the entire training/validation base, but for the random sample of them. This results in substantial oscillations of the specified curve even after the very high number of epochs.

The main stimulus for development of the molecular dynamics potentials that provide the results similar to DFT, is the attempt to reduce the calculation time. For this reason it is important to pay attention to the duration of calculations, except for the accuracy. Dependence of time to do one step of molecular dynamics in the LAMMPS software on the potential type (DP-e2 or GAP) an the used hardware is given in fig. 3. The dependences given in the figure are close to linear ones. The calculations were done for a series of graphene models with the adsorbed lithium produced by translation of the estimated cell $C_{98}Li_3$. The minimum from the considered system contained 404 atoms. Testing was done on computers with Intel i9 10980XE (18-core) and AMD EPYC 7742 (64-core) processors. Calculations with the DP potential were additionally started on NVIDIA Tesla P100 (16 GB video memory), Titan V (12 GB video memory) and Tesla

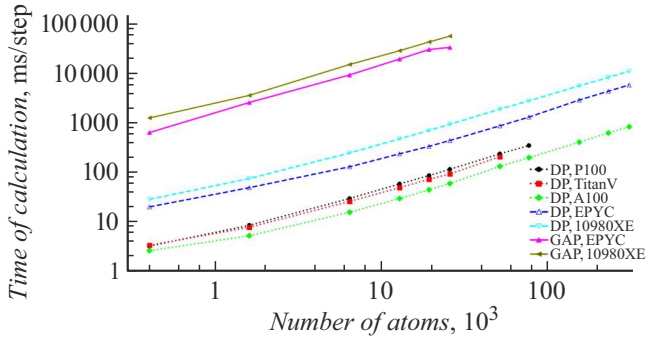

Figure 3. Time to do one step of molecular dynamics when using various hardware (logarithmic scale of axes).

A100 (80 GB video memory) video cards. From fig. 3 you can see that the calculations using the GAP potential take dozens of times more time that the calculations with the DP potential on the same processor. Compared to the launch of the calculation on a graphic accelerator, the loss in time is measured in hundreds of times now. On the background of such significant changes in the calculation time the differences in the calculation time on different video cards and processors do not seem substantial. Due to the high requirements to the computing resources, the GAP potential was only tested in relatively small systems — up to 25 856 atoms. Despite relatively low requirements to the computing resources for the DP potential, in the case of using the graphic accelerators the maximum size of the system available for modeling turns out to be limited by the size of the video memory, which is usually much smaller than the random access memory of the central processor. From fig. 3 you can see that for NVIDIA Titan V video cards the available models are models of up to 50 000 atoms. For Tesla P100 video card this value is several times higher and is 70 000 atoms. Models from more than 310 000 atoms may be studied on Tesla A100 video cards. Besides, the time for calculation of one step in such a model will be three orders less than the time of one step of molecular dynamics in the VASP package for model $C_{98}Li_3$.

Summing up the above estimates of the accuracy of the obtained potentials (table 2) and the computing resources they require (fig. 3), one may conclude that using of the GAP potential is not justified even in the case when it is not possible to do the calculations with the DP potential on graphic accelerators. If there is such a possibility, it is not feasible to do the calculations with the DP potential on the central processor.

2.3. Applied software

Apart from using the DP potentials in the LAMMPS software, they may be incorporated quite easily into the user software in Python by deepmd module. Based on GUI4dft software [30] developed by the author previously, the graphic shell was developed to calculate the energies of the systems with the DP potentials, including those obtained in this paper. The software is available to the public on the GitVerse platform (https://gitverse.ru/sozykin/ml-potential-calculator). It may be used to assess the energies of the systems specified in the VASP POSCAR format, and to assess quantitatively the degree of the system difference using the SOAP descriptor. The latter possibility is available through quippy module.

The graphic interface of the software is given in fig. 4. On „Settings“ insert the user specifies the path to the used DP potential. On „Model“ insert there is a button to select a file with atomic structure in the POSCAR format and forms where information is displayed on the model handled at the moment. On „Calculation“ insert there are tools for calculation of the energies of the model or SOAP descriptor. Since the SOAP descriptor is a vector of a large number of elements, its values are hard to perceive. The tools available in the software enable calculations of the norm for the difference in the descriptors of the systems previously opened in the software. This parameter may be used as the measure of the system difference.

Let us consider the example of the software use. Compare the energies of lithium adsorption calculated by different methods. For all non-equivalent centers of adsorption in the studied systems the energies of lithium adsorption were calculated within DFT and with the DP potential using formula

$$E_{ads} = E_{model+\mathrm{Li}} - E_{model} - E_{\mathrm{Li}},$$

where $E_{model+\mathrm{Li}}$ — energy of the estimated cell of nanotube, graphene, biphenylene, irida-graphene, ψ-graphene or tetra-penta-deca-hexagonal graphene with one lithium atom, E_{model} — energy of the estimated cell of the same model without the lithium atom, E_{Li} — energy of the lithium atom. Equilibrium positions of the lithium atom are located above the centers of the carbon rings of the surface. Let us first provide the results of DFT. For all the studied systems the surfaces contain six-member cycles, but the adsorption energies in them vary: they are equal to −1.62, −1.76, −2.19, −2.27, −2.49 and −2.50 eV for graphene, CNT, biphenylene, irida-, tetra-penta-deca-hexagonal and ψ-graphene accordingly. The produced energies of adsorption hardly depend on the carbon ring size except for the case of adsorption in a three-member cycle of irida-graphene, where the adsorption energy is −1.97 eV. In the order of increase of the size of the carbon ring, above which the lithium atom is adsorbed: biphenylene (−2.10, −2.19, −2.11 eV), irida-graphene (−1.97, −2.27, −2.29 eV), ψ-graphene (−2.52, −2.50, −2.55 eV), tetra-penta-deca-hexagonal graphene (−2.43, −2.50, −2.49, −2.51 eV).

For the equilibrium configurations found in DFT, the energies were calculated with the DP potential, and the interaction energies were calculated. The least average error in the different centers of adsorption in the interaction energy was obtained for tetra-penta-deca-hexagonal graphene (0.05 eV), and the maximum one — for the nanotube

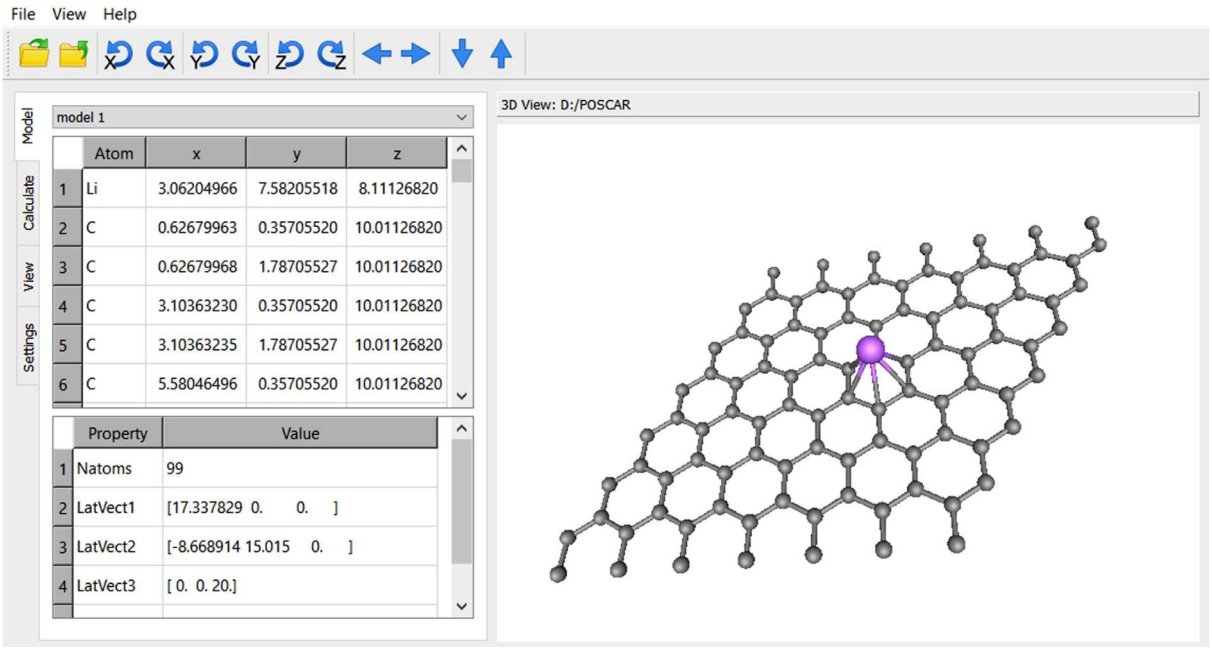

Figure 4. Applied software interface.

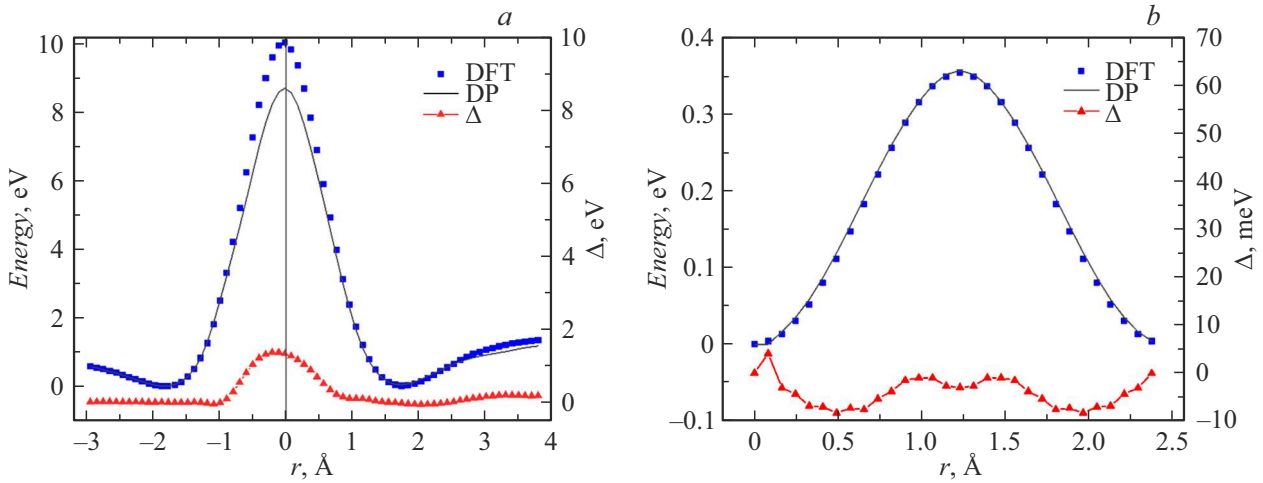

Figure 5. DFT- and DP-energies, their difference for test sets: *a* — 1, *b* — 2.

(0.32 eV). Therefore, for this parameter the error does not exceed 20 %.

When the DP potential is used, RMSE of energy for two test data sets described above made 4.75 meV/atom (95 meV/Å) and 3.35 meV/atom (20 meV/Å) for sets 1 and 2 accordingly. To determine the areas of test sets, for which the largest error was obtained, let us see the energy profiles given in fig. 5. Energies were counted relative to the minimum value independently for each line. Besides, for the test set 1 the absolute values in the minima are practically same, and for the test set 2 the DFT data are shifted relative to the DP data by the value approximately equal to 0.33 eV. This is the shift reflected in RMSE. The third line (Δ) — difference of relative energies for DFT and DP. Relative energies for the test set 2 are close everywhere. The large RMSE for the first set is related to large errors in the energy for the lithium positions near the nanotube surface. Such positions are far from those, which were used for training, and those that may be observed in the experiment.

Conclusion

In process of the study a base was developed, which contains data on the energies of more than 8700 configurations of the carbon nanomaterial structures with lithium atoms. Configurations arose in process of molecular-dynamic modeling at temperatures of up to 450 K.

Comparison of two approaches to training of potentials of interparticle interaction and various descriptors within each of them showed that the most effective was the potential obtained by the deep training method with a two-particle descriptor, which takes into account the relative position of two atoms.

The ability to describe the barriers of lithium diffusion on the carbon surface with high accuracy was demonstrated, as well as the energies of the complexes with lithium when located at typical distances from the carbon surface.

Comparison of the energies of lithium atom interaction with the carbon surface calculated within the electronic density functional theory and with the help of the obtained potential demonstrated that the accuracy of this value determination turns out to be especially high (less than 0.2 eV) for the case of adsorption on graphene. The maximum error (0.8 eV) was recorded for the case of adsorption on irida-graphene. Specified errors, however, do not exceed the specific spread of this value when using various first-principle tools.

Conflict of interest

The author declares that he has no conflict of interest.

References

[1] Z. Wu, K. Sun, Z. Wang. Batteries, **8**, 246 (2022).
[2] P. Lian, X. Zhu, S. Liang, Z. Li, W. Yang, H. Wang. Electrochim. Acta, **55** (12), 3909 (2010).
[3] L.A. Montoro, E.Y. Matsubara, J.M. Rosolen. J. Power Sources, **257**, 205 (2014).
[4] C.E. Nwanno, W. Li. Nano Res., **16** (11), 12384 (2023).
[5] M.W. Ochapski, D. Ataç, J.G.M. Sanderink, A.Y. Kovalgin, M.P. de Jong. Carbon Trends, **4**, 100045 (2021).
[6] Y. Zhong, K. Deng, J. Zheng, T. Zhang, P. Liu, X. Lv, W. Tian, J. Ji. J. Mater. Sci. Technol., **149**, 205 (2023).
[7] Y. Zhou, R. Chen, Z. Gao, J. He, X. Li. Mater. Today Energy, **37**, 101389 (2023).
[8] X. Yan, Z. Fu, L. Zhou, L. Hu, Y. Xia, W. Zhang, Y. Gan, J. Zhang, X. He, H. Huang. ACS Appl. Mater. Interfaces, **15** (14), 17986 (2023).
[9] A.P. Bartók, M.C. Payne, R. Kondor, G. Csányi. Phys. Rev. Lett., **104** (13), 136403 (2010).
[10] A.V. Shapeev. Multiscale Model. Simul., **14** (3), 1153 (2016).
[11] J. Han, L. Zhang, R. Car, E. Weinan, Commun. Comput. Phys., **23** (3), 629 (2018).
[12] B. Deng, P. Zhong, K.J. Jun, J. Riebesell, K. Han, C.J. Bartel, G. Ceder. Nat. Mach. Intell., **5** (9), 1031 (2023).
[13] V.L. Deringer, G. Csányi. Phys. Rev. B, **95** (9), 094203 (2017).
[14] P. Rowe, V.L. Deringer, P. Gasparotto, G. Csányi, A. Michaelides. J. Chem. Phys., **153** (3), 034702 (2020).
[15] T. Kocabaş, M. Keçeli, A. Vázquez-Mayagoitia, C. Sevik. Nanoscale, **15** (19), 8772 (2023).
[16] H. Muhli, X. Chen, A.P. Bartók, P. Hernández-León, G. Csányi, T. Ala-Nissila, M.A. Caro. Phys. Rev. B, **104** (5), 054106 (2021).
[17] Y. Wang, Z. Fan, P. Qian, T. Ala-Nissila, M.A. Caro. Chem. Mater., **34** (2), 617 (2022).
[18] J. Wang, H. Shen, R. Yang, K. Xie, C. Zhang, L. Chen, K.M. Ho, C.Z. Wang, Z. Cai, S. Wang. Carbon, **186**, 1 (2022).
[19] S. Fujikake, V.L. Deringer, T.H. Lee, M. Krynski, S.R. Elliott, G. Csányi. J. Chem. Phys., **148** (24), 241714 (2018).
[20] L. Zhang, H. Wang, M.C. Muniz, A.Z. Panagiotopoulos, R. Car, E. Weinan. J. Chem. Phys., **156** (12), 124107 (2022).
[21] G. Kresse, J. Furthmuller. Phys. Rev. B, **54**, 11169 (1996).
[22] I.V. Lebedeva, A.V. Lebedev, A.M. Popov, A.A. Knizhnik. Comput. Mater. Sci., **128**, 45 (2017).
[23] S. Klawohn, J.P. Darby, J.R. Kermode, G. Csányi, M.A. Caro, A.P. Bartók. J. Chem. Phys., **159**, 174108 (2023).
[24] V.L. Deringer, A.P. Bartók, N. Bernstein, D.M. Wilkins, M. Ceriotti, G. Csányi. Chem. Rev., **121** (16), 10073 (2021).
[25] Y. Shaidu, E. Küçükbenli, S. De Gironcoli. J. Phys. Chem. C, **122** (36), 20800 (2018).
[26] Y. Zhang, H. Wang, W. Chen, J. Zeng, L. Zhang, H. Wang, E. Weinan. Comput. Phys. Commun., **253**, 107206 (2020).
[27] S. Trillot, J. Lam, S. Ispas, A.K.A. Kandy, M.E. Tuckerman, N. Tarrat, M. Benoit. Comput. Mater. Sci., **236**, 112848 (2024).
[28] M. Fronzi, R.D. Amos, R. Kobayashi, N. Matsumura, K. Watanabe, R.K. Morizawa. Nanomaterials, **12**, 3891 (2022).
[29] S.K. Achar, L. Zhang, J.K. Johnson. J. Phys. Chem. C, **125** (27), 14874 (2021).
[30] S.A. Sozykin. Comput. Phys. Commun., **262**, 107843 (2021).

Translated by M.Verenikina